# Influence of Rib Cortical Bone Age on Human Body Model Probabilistic Rib Fracture Risk Predictions

Karl-Johan Larsson, Johan Iraeus

***Abstract*** Strain-based, probabilistic, rib fracture risk prediction using human body models (HBMs) commonly represents age effects only through modulation of fracture risk functions, while rib cortical bone material properties are kept constant. This study investigated the effect of also age-adjusting the cortical material model parameters on the rib fracture risk prediction, and the representativeness of such models given substantial inter-individual variability. Age-trends in tensile and compressive rib cortical bone stress–strain curves (17–99 years) were characterised using principal component analysis and regression, enabling age-specific material curves and stochastic representation of individual variability around age trends. Resulting material properties were implemented in SAFER HBM and evaluated in rib bending tests and pendulum chest impact tests. Including age effects in the material definition altered structural response and fracture risk predictions compared to applying age adjustment only in the risk function, producing lower risks for younger, and higher risks for older ages. Representation of inter-individual material variability at different ages resulted in wide and skewed risk distributions, where the age-specific material parameters resulted in median rather than mean risks. Cortical bone material ageing and age-dependent risk functions address complementary aspects of rib fracture risk prediction and should be considered jointly in HBM-based assessments.
***Keywords*** Ageing, Human body model, Rib cortical bone, Rib fracture risk, Strain-based injury prediction.

## I. INTRODUCTION

The thorax is a commonly injured body region in low-to-high severity vehicle crashes, with rib fractures being particularly prevalent and strongly associated with increasing age [1–5]. Car safety systems have traditionally been designed and evaluated by crash testing with the injury risk assessed using anthropomorphic test devices (ATDs), which commonly estimate thoracic injury risk based on chest deflection. How well the chest deflection estimated risk correlates with occupant injury risk in real-life crash scenarios has been questioned [6–8].

As an alternative to ATDs, finite element human body models (HBMs) can be used to represent occupants in virtual simulations of crashes. In contrast to ATDs, HBMs, such as SAFER HBM [9], THUMS [10], VIVA+ [11] and GHBMC [12–13], model the human anatomy in greater detail, including individual ribs. With this detailed representation, there is a potential of HBMs to predict rib fractures at the tissue level, using physical parameters that are related to the fracture mechanism, such as stress or strain.

In particular, rib cortical strain has been shown to correlate with rib fractures in post mortem human subject (PMHS) testing [14]. Thus, strain-based fracture risk functions have been proposed [15–17]. In [17] the authors developed a risk function based on failure strains from PMHS rib cortical bone tensile tests, and showed that age was a significant covariate, reducing the failure strain by 12% per decade of ageing. The reduced failure strain in rib cortical bone with increasing age can partly explain the increasing rib fracture risk observed with age.

In addition to failure strain, Young's modulus and yield stress are also significantly reduced with ageing as evident from analysis of PMHS rib cortical bone tensile mechanical properties [18]. No significant monotonic trends for mechanical properties with age were identified for compressive properties, but there were indications of a non-linear trend, with properties initially increasing up until the thirties and then decreasing again with increasing age [19]. For both loading modes, substantial inter-individual variability remains also after controlling for age. Previous analyses of age trends focused on scalar parameters derived from the stress-strain curves, and not on curves themselves. As a stress-strain curve simultaneously describes elastic, yield, and post-yield behaviour, additional age-related trends may be identified when the whole curve is analysed.

In previous work, HBMs have been modified to represent elderly occupants. For representation of elderly ribs, modifications included changes in rib morphology, scaling of the cortical bone thickness, and reducing the mechanical properties for the rib cortical bone [20–22]. In TABLE I, Young's modulus and yield stress values that were selected to represent the material properties of 70 years old (YO) rib cortical bone in HBMs are presented,

K. Larsson (e-mail: karl-johan.larsson@autoliv.com) is a Biomechanics Manager at Autoliv Research, Vårgårda, Sweden. J. Iraeus is a Researcher at the Department of Mechanical Engineering at Chalmers University of Technology, Gothenburg, Sweden.

reflecting a wide range of material properties.

TABLE I
RIB CORTICAL BONE MATERIAL PARAMETERS REPRESENTING 70 YO MATERIAL IN PREVIOUS WORK

| Source | Young's modulus [GPa] | Yield stress [MPa] |
|---|---|---|
| *Schoell et al.* [21] | 11.5 | 88 |
| *Jin et al.* [20] | 9.8 | 97 |
| *von Kleeck et al.* [22] | 13.9 | 76 |

The potential of HBMs to represent human occupants and injury risk is recognised by consumer safety organisations. Euro NCAP will include crash simulations with HBMs as part of the occupant protection assessment [23]. As a first step, strain-based rib fracture risk predictions at ages 25, 50, and 75 years are performed in the Euro NCAP procedure for HBM certification [24–25]. Notably, the age adjustment in this evaluation is currently limited to adjusting the strain-based risk functions, while rib cortical bone material properties remain constant.

As rib cortical bone material properties strongly influence strain-based fracture risk predictions [26] and age-specific strain-based rib fracture risk prediction is a potential criterion for HBM-based vehicle safety assessment, there is a need to further examine the effect of age-adjusted rib cortical bone material properties on HBM rib fracture risk predictions. As age only explains part of the variability in material properties, it is also of interest to understand if age-specific material properties result in risk predictions that are representative of the population risk at the targeted age. As strain-based risk functions are non-linear [17], age-averaged material properties do not necessarily result in average fracture risk predictions [27].

To support future HBM-based assessment criteria and studies of age effects on rib fracture risk prediction, the primary objective of this study is to investigate the effect of age-adjusting cortical bone material properties beyond failure strain when performing probabilistic rib fracture risk prediction with HBMs. A secondary objective is to assess whether age-averaged material properties yield fracture risk predictions that are representative of population-level risk, given the substantial inter-individual variability observed in experimental data.

To address these objectives, age effects were modelled in two ways: (1) partial age adjustment, where only the reduction in failure strain was considered through the age covariate in the injury risk function, and (2) full age adjustment, where all cortical bone material properties affected by age trends (e.g. Young's modulus, yield stress, plastic hardening) were modified along with the age effect in the injury risk function. Predicted rib fracture risks were compared between these two. Furthermore, fracture risks predicted from material properties representing the inter-individual variability at different ages were compared to risks from age-specific material properties.

## II. METHODS

Age-dependent rib cortical bone material behaviour was modelled by applying principal component analysis (PCA) to experimental tensile and compressive stress–strain curves, followed by regression of principal component (PC) scores against donor age to model age trends. Next, these regression trends were used to generate age-specific stress–strain curves, while regression residuals were used to represent the inter-individual variability around these age trends. Generated curves were implemented in an LS-DYNA (R12.2 MPP, Ansys Inc., Canonsburg, Pennsylvania, 16 CPUs) material model, and applied to the ribs of 50$^{th}$ Male SAFER HBM v11.1 [9][28]. The influence of age-specific material properties and material variability on strain-based rib fracture risk prediction was finally evaluated in simulations of two scenarios: a component level rib bending test and a pendulum chest impact test.

### *Rib Cortical Bone Material Test Data*

The rib cortical bone reference data used in this study was stress-strain curves from tensile and compressive testing of PMHS rib cortical bone samples at two different loading rates. The testing and resulting material properties derived from the stress-strain curves was previously reported in [18] for the tensile tests and in [19] for compressive tests. In both studies, two targeted strain rates were used, 0.5 strain/s (Fast) and 0.005 strain/s (Slow). While Fast loading is representative for highly strained rib regions in crashes, rib deformation is spatially non-uniform and elements experience a range of local strain rates. Therefore, also Slow-rate data were included for material modelling. Coupons for the tensile testing [18] were harvested from N = 61 donors (17-99 years old; YO), but not all donors had material samples successfully tested at both Fast and Slow rates. Therefore, only N =

58 Fast and N=58 Slow stress-strain curves were used for the current analysis. Compressive stress-strain curves [19] were obtained with samples from N=30 donors (18-95 YO) at both Fast and Slow rates. All curves were re-computed to true stress and true strain for later use in LS-DYNA material modelling and are shown in Fig. 1.

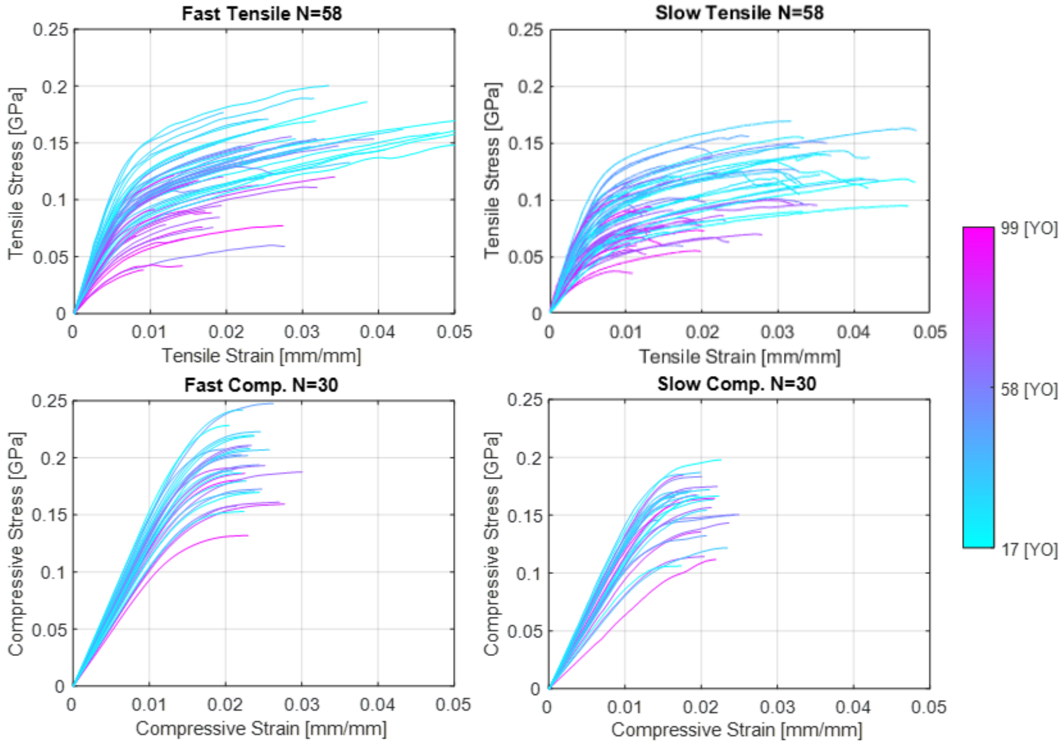


Fig. 1. Rib cortical bone true stress and true strain curves from testing [18–19], including number of samples (N). Upper left: Fast tensile, Upper right: Slow tensile, Lower left: Fast compressive, Lower Right: Slow compressive. Curve colour mapped to age of donor according to legend.

***Modelling Age Trends using PCA and Regression***

All curves were re-sampled to 500 stress-strain points. For each test configuration (e.g. tensile Fast) the data were sorted into a matrix for PCA analysis. Each row in the matrices was one re-sampled stress-strain curve, with the first columns containing the stress values (ordered by corresponding strain values) and the following columns containing the 500 strain points. Stress and strain were normalised separately (by their corresponding averages) to avoid dominance of either variable in the PCA due to differing physical units. The PCA and regression modelling was performed using MATLAB (R2023a, Statistics and Machine Learning Toolbox v.12.5, The MathWorks, Natick, Massachusetts).

The first N principal components (PCs), together describing more than 95% of variability in curves, were kept for regression modelling. Three different regression models were considered: linear regression, linear regression with second order terms (quadratic), and Gaussian Process Regression (GPR, default parameter settings) to capture potential non-linear trends in curve shape with age. The regression model (linear, quadratic, or GPR) producing the lowest average root-mean-squared error (RMSE) under leave-one-out cross-validation was selected to represent the age trend.

With regression models predicting PC scores, corresponding age-representative stress–strain curves were reconstructed using corresponding PCs. From stress-strain curves predicted for any age, material properties including Young's modulus, yield stress and yield strain were extracted using the same method as in the original experimental studies [18–19] for later use in material modelling. Additionally, residuals in terms of predicted Young's modulus vs. Young's modulus from original test curves were computed for reference in the next step.

**Representing Individual Variability around the Age Trends**

A sampling method that generated stress-strain curves for a synthetic individual of any given age was created. As several PMHS donors had both Slow and Fast tests performed, potential correlation between Fast and Slow PC scores for the individuals tested at both rates was investigated (separately for tensile and compressive curves, as initial analysis indicated no correlation between tensile and compressive PC scores). Significance for correlations were judged by $\alpha < 0.05$ (Student's t-test, corcoef function MATLAB).

Random Fast PC scores (tensile and compressive) were selected from normal distributions with age-predicted PC scores as mean and standard deviation (SD) corresponding to the SD of residuals from PC score age regressions (assuming normally distributed residuals, verified through visual inspection). Next, corresponding Slow PC scores were sampled from conditional normal distributions specified by Fast PC score and corresponding correlations. Initial analysis indicated that random combinations of PC scores in extreme cases resulted in non-physical stress-strain curves (e.g., negative Young's modulus). Therefore, to exclude non-physical realisations while preserving experimentally observed variability, randomly generated curves were accepted only if the resulting Young's modulus lay within ±2 SD of the regression residual distribution. Samples of stress-strain curves generated by the above method were used to represent synthetic individuals for various ages.

***Computational Material Model and Strain Rate Calibration***

To represent the tension and compression asymmetric mechanical properties of rib cortical bone [19], the LS-DYNA material model *MAT_PLASTICITY_COMPRESSION_TENSION (MAT_124) was selected. This material model allows asymmetric elastic–plastic behaviour in tension and compression but is in other aspects similar to the baseline HBM material model (MAT_24). Young's modulus for each loading direction was selected as the average of Fast and Slow predicted results. This averaging represents a modelling compromise across strain rates, as MAT_124 does not permit strain rate effects for Young's modulus. The post-yield portions of the generated stress-strain curves were used to define stress versus effective plastic strain. Stress curves were taken from the predicted Fast result (0.5 strain/s is a representative rate for crash loading, [19]) and were truncated such that the final two points ensured a positive tangent modulus during extrapolation (LS-DYNA default behaviour is to extrapolate if strain goes beyond provided curves).

Age independent strain rate effects on the yield surface were implemented using Cowper–Symonds scaling and yield stress scale factors (scaling yield stress to a corresponding quasistatic magnitude). These parameters were manually calibrated by simulating uniaxial tensile and compressive material tests at three rates: quasistatic (Cowper–Symonds scaling disabled), 0.005 strain/s, and 0.5 strain/s. Agreement between simulated and experimental stress–strain curves was assessed qualitatively by visually comparing elastic stiffness, yield stress, and post-yield hardening behaviour across decades of ages (20–90 YO), strain rates, and loading modes. Qualitative assessment was chosen as reference data were not equally distributed across ages, leading to difficulties designing a quantitative metric that was balanced across ages.

***Effect of Age-adjusted Material Modelling on Rib Fracture Risk Prediction***

The effect of partial vs. full age adjustment on rib fracture risk predictions was evaluated in two scenarios, a component level single rib bending test, and a pendulum impact to the chest. Representativeness of risks from age-specific material properties, in relation to risks from material properties representing population variability, was evaluated in a pendulum impact scenario.

A strain-based risk function including age as a covariate [17] was used to calculate rib fracture risk in all simulations, and the age parameter in the risk function was always set to the age of interest. The first principal strain, in the middle element layer, was extracted from all elements in the rib cortical bone at 0.2 ms increments, and the maximum value across the cortex for each rib (i.e., 100$^{th}$ percentile) was used for risk calculations. A Poisson-Binominal distribution as proposed in [15] was used to compute the combined risk of X or more fractured ribs (NFRX+) in the rib cage.

**Material Age Effect on Rib Bending Test**

The sixth rib of SAFER HBM was used in simulations of a rib bending test (ribs bent through anterior-posterior compression, see Fig. 2 and [29] for description of test setup). The boundary condition models, including models of rib potting and prescribed velocity of the anterior end were previously presented in [30].

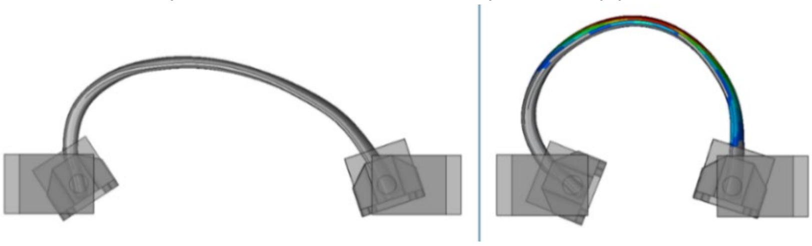

Fig. 2. Simulation model of rib bending test. Left: initial configuration. Right: deformed configuration.

Two evaluations were conducted to study how material age affect force and displacement to fracture. In the first, full age adjustment of material properties was implemented, and age was varied from 19–99 YO, in two-year increments. Fracture was determined when rib fracture risk met 50% risk, and current rib displacement (as % of initial span length) and boundary condition force were recorded. In the second, partial age adjustment was implemented by fixing the material properties to 45 YO, and only the risk function was adjusted to the evaluated ages.

**Material Age Effect on Pendulum Impact**

The boundary condition model for Kroell *et al.* 1971 (OpenVT v.1.0.0) as used in Euro NCAP HBM qualification [25] was used but with varied initial velocity of the impactor. The torso of SAFER HBM (legs, arms, and head were removed to save computational time – the focus of study was relative risk effects) was impacted by a 23.4 kg cylindrical pendulum centred at the sternum between 3rd and 4th rib levels, see Fig. 3. The impact direction was anterior-posterior and initial pendulum velocity was set to 4.0, 5.0, and 5.5 m/s. For the full age adjustment, ages of 25, 45, and 65 YO were used and risk of two or more fractured ribs (NFR2+) and NFR3+ rib fracture risks were calculated. For the partial age adjustment, the material properties were fixed at 45 YO while fracture risks were calculated also at 25 and 65 YO to compare resulting risks to those with age-specific material properties.

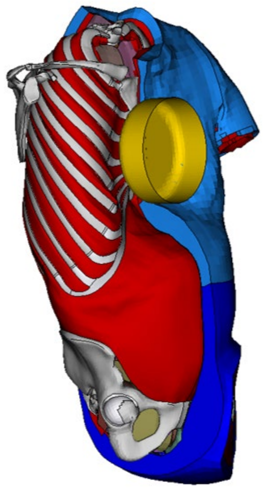

Fig. 3. Pendulum impact to torso of SAFER HBM. External skin and muscle model layer hidden on right-hand side to show rib cage.

**Representativeness of Age-specific Material**

Here, the pendulum impact condition was used with 5.5 m/s initial velocity. Three simulations with full age adjustment to 25, 45, and 65 YO were conducted. In addition, population samples with N=50 random material configurations representing individual variability at each corresponding age were simulated. Risks of NFR2+, NRF3+, and NFR4+ were calculated and age-specific risks were compared to mean and median of corresponding sets of risks from population samples at the different ages.

## III. RESULTS

***Modelling Age Trends using PCA and Regression***

Variance explained for the first PCs is in Table II. For all four test configurations, the first two PCs together explained ≥98.8% of the total variance; therefore, further analysis was restricted to include only the first two PCs.

Table II
Variance explained and cumulative variance explained from PCA of stress-strain curves across the four configurations (rounded to 1 decimal)

| | Fast Tensile | | Slow Tensile | | Fast Compressive | | Slow Compressive | |
|---|---|---|---|---|---|---|---|---|
| PC | Var. expl. [%] | Cumul. | Var. expl. [%] | Cumul. | Var. expl. [%] | Cumul. | Var. expl. [%] | Cumul. |
| 1 | 85.3 | 85.3 | 84.8 | 84.8 | 62.5 | 62.5 | 57.7 | 57.7 |
| 2 | 14.4 | 99.7 | 14.8 | 99.6 | 36.8 | 99.3 | 41.1 | 98.8 |
| 3 | 0.3 | 99.9 | 0.3 | 99.9 | 0.6 | 100.0 | 1.1 | 99.9 |
| 4 | 0.0 | 100.0 | 0.1 | 99.9 | 0.0 | 100.0 | 0.1 | 100.0 |

The modes of stress-strain curve shape represented by corresponding PCs are demonstrated in Fig. 4 for Fast tensile and Slow compressive PC results by modulating PC-score within ±2 SDs of corresponding subject scores. Slow tensile and Fast compressive corresponding PCs had similar effects on curve shape.

In Fig. 5, examples of PC scores from individual subjects as well as representative predictions from fitted regression models are shown. For tensile PCs (Fast and Slow), GPR models obtained lowest root-mean-squared error (RMSE) among the evaluated regression models and for compressive PCs, quadratic regression models had the lowest RMSE. Notably, there is substantial residual variability around the predicted age trends.

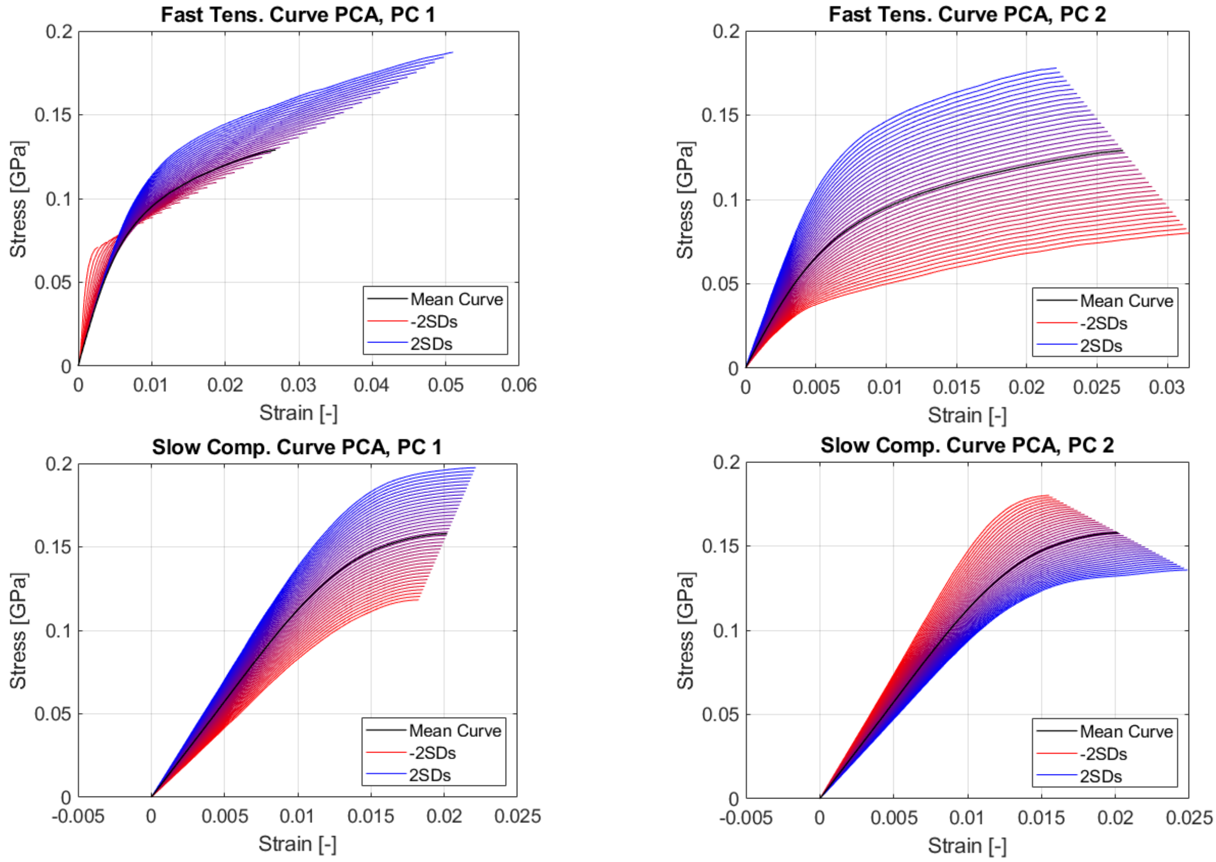


Fig. 4. Effect of PC on stress-strain curve shape. Upper row shows effect of PC 1 and PC2 on Fast Tensile stress-strain curves. Lower row shows effect of PC1 and PC2 on Slow Compressive stress-strain curves.

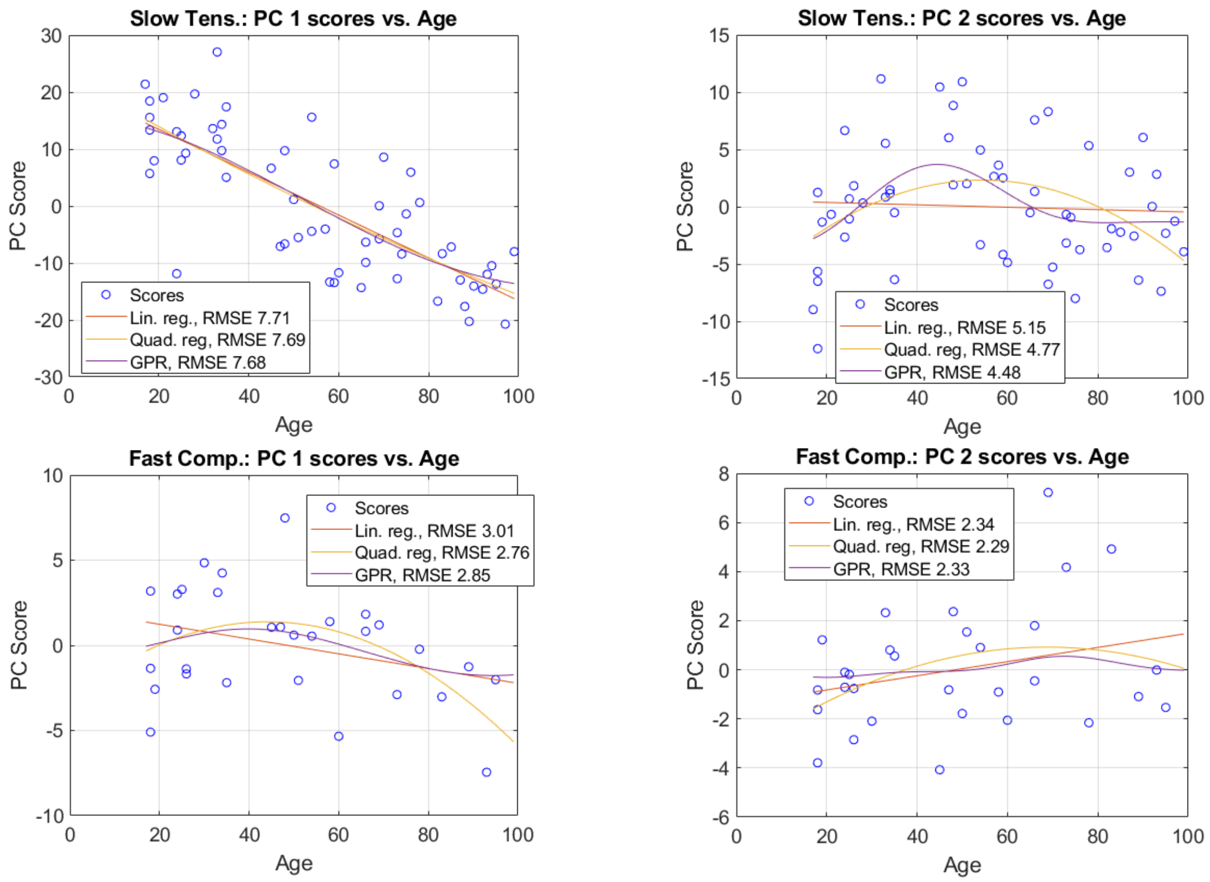


Fig. 5. PC scores vs. Age (YO) and predictions of fitted regression models, linear (Lin.), quadratic (Quad) and GPR. Upper row shows scores and predictions for Slow tensile PCs. Lower row shows scores and predictions for Fast compressive PCs.

Using the regression models, corresponding stress-strain curves were predicted for specified ages. Young's modulus was computed from predicted curves. Regression residual SD of Young's modulus was computed against Young's modulus from test curves. Fig. *6* shows these as lines over age. The individual test subject moduli are also displayed to allow visual inspection of fit.

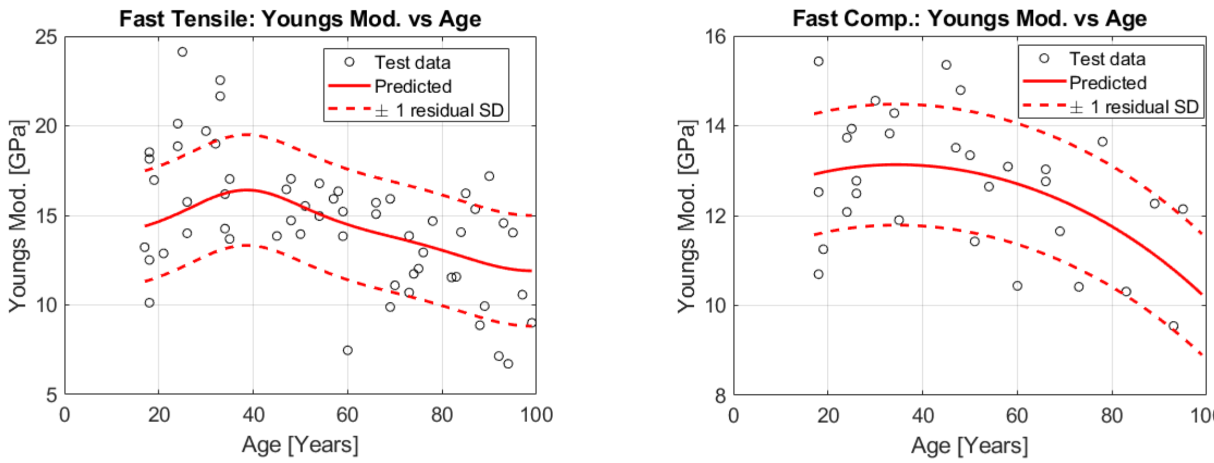


Fig. 6. Young's modulus vs. age from test data and predicted stress-strain curves (PC score regressions). Left: Modulus from Fast tensile stress-strain curves. Right: Modulus from Fast compressive stress-strain curves.

**Representing Individual Variability around Age Trends**

For stress-strain curves from donors tested in both Fast and Slow rates, there were significant correlations identified in terms of PC score magnitudes between the loading rates (tensile: Fast PC 1 - Slow PC 1: $\rho = 0.70$, $p < 0.001$; Fast PC 2 - Slow PC 2: $\rho = 0.70$, $p < 0.001$. Compressive: Fast PC 1 - Slow PC 1: $\rho = 0.51$, $p = 0.004$; Fast PC 1 - Slow PC 2: $\rho = -0.50$, $p = 0.005$), see Appendix A. A sample of N=50 randomly generated Fast and Slow stress-strain curves at 25 YO is shown in Fig. 7, together with corresponding physical test results from donors within ± 5 years.

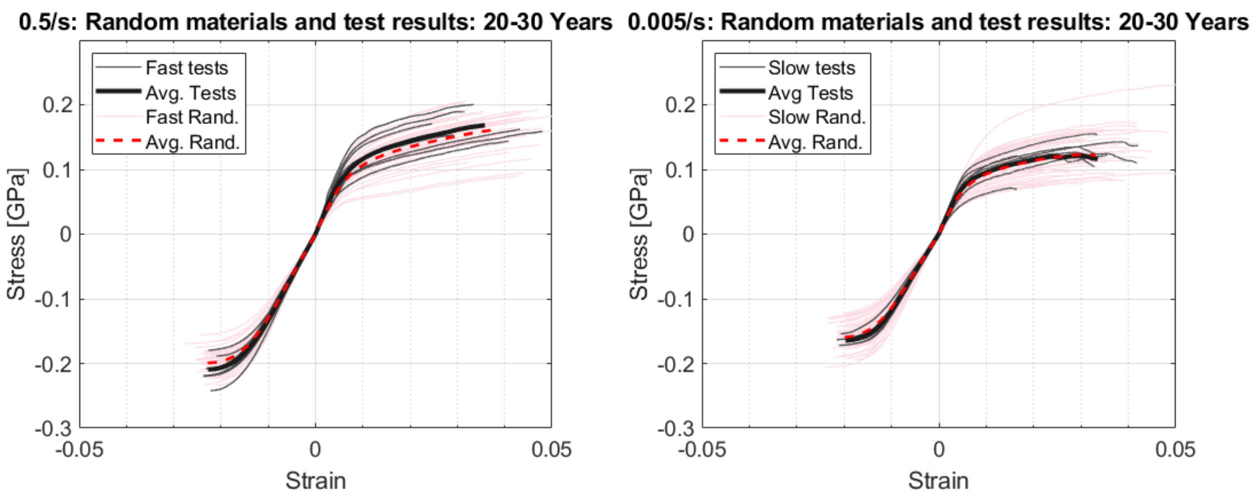


Fig. 7. Tensile and compressive stress-strain curves. N=50 randomly generated at 25 YO together with corresponding test curves [18–19] from donors (20–30 YO). Left: Fast loading rate, Right: Slow loading rate.

## Computational Material Model and Strain Rate Calibration

Cowper-Symonds rate scale parameters were calibrated to C = 2.4 and P = 4.0. Scale factors for stress vs. plastic strain curves were 0.79 for tensile and 0.75 for compressive.

Examples of predicted stress-strain results from the calibrated material model can be seen for different ages and strain rates in Fig. 8 and Appendix B, together with corresponding test curves from similar ages (± 5 years), demonstrating an overall good alignment across ages and strain rates.

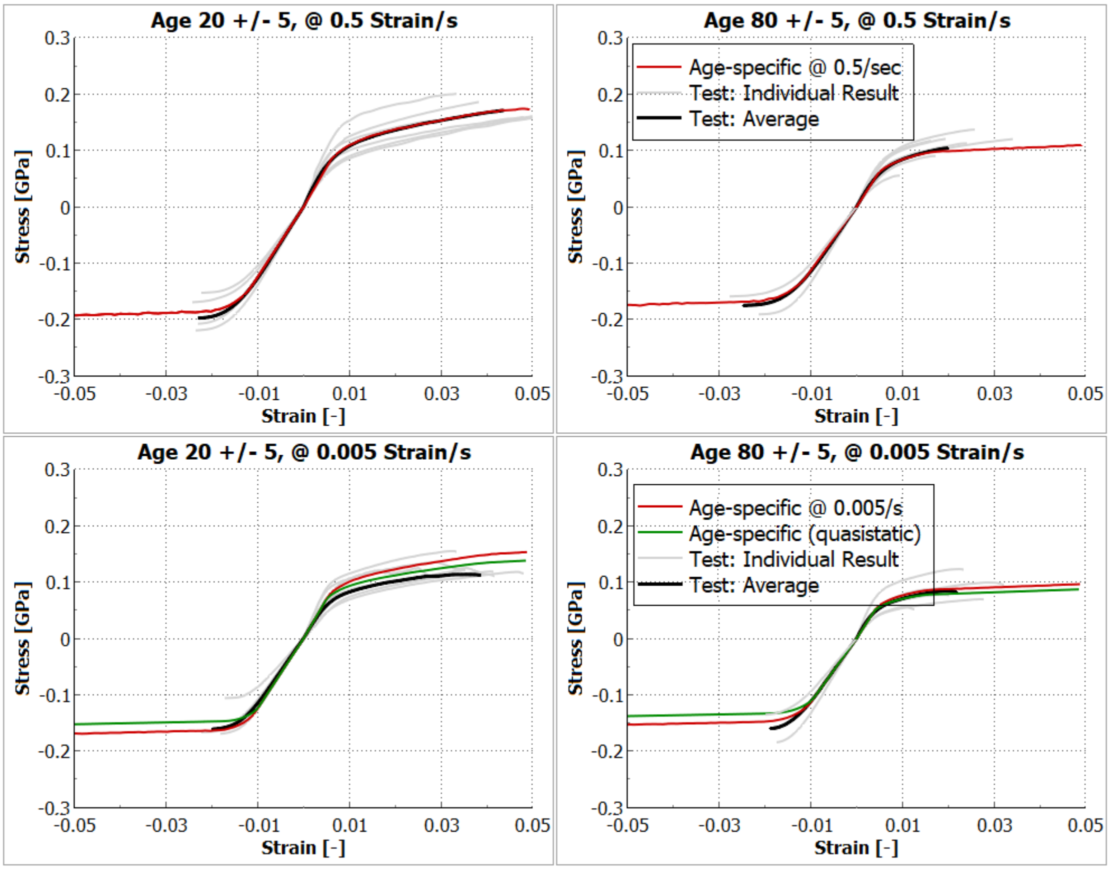


Fig. 8. Tensile and compressive stress-strain curves computed from age-specific material properties at 20 and 40 YO, including test curves from ± 5 years [18–19]. Top: Fast, bottom: quasistatic and Slow.

### *Effect of Age-adjusted Material Modelling on Rib Fracture Risk Prediction*

**Material Age Effect on Rib Bending Test**

In the rib bending test, displacement to fracture was reduced from 36% to 18% (50% decrease) for the partial age adjustment as age varied from 19–99 YO. For full age adjustment the fracture displacement was reduced from 40% to 17% (58% decrease), Fig. 9. Force to fracture was reduced from 86 N to 72 N (16%) for partial age adjustment and from 91 N to 53 N (42%) for full age adjustment, Fig. 9.

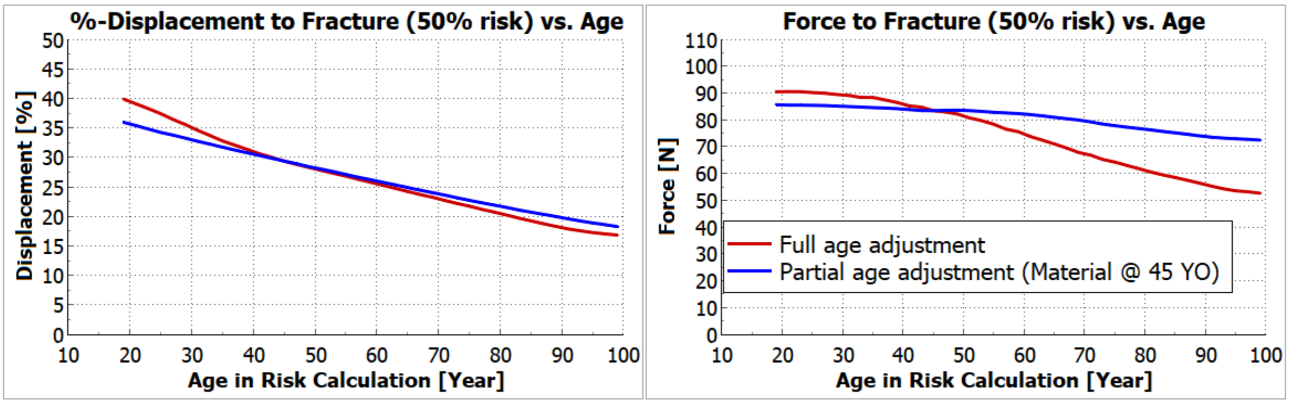


Fig. 9. Displacement (%-initial span length) (left) and force (right) to fracture (50%) risk for ages 19–99 YO. Red curves used full age adjustment and blue curves used partial age adjustments.

**Material Age Effect on Pendulum Impact**

For pendulum impact rib fracture risks, the partial age adjustment systematically produced higher predicted risks for younger ages and lower predicted risks for older ages, when compared to those with full age adjustment, TABLE III. The exception was when risk was saturated at 0% or 100%. As a notable example, for 4 m/s pendulum speed, the 45 YO material predicts 9.6% risk of NFR2+ with age set to 65 YO in the risk function (which is the partial age adjustment). Using full age adjustment in the same calculation results in a prediction of 30.4% NFR2+

risk, tripling the risk magnitude.

TABLE III.
RISK OF NFR2+ AND NFR3+ AT DIFFERENT AGES, AGE-ADJUSTED MATERIAL PROPERTIES, AND INITIAL PENDULUM VELOCITIES. FOR 45 YO MATERIAL RISKS WERE COMPUTED ALSO AT 25 YO AND 65 YO (PARTIAL AGE ADJUSTMENT). BOLD VALUES INDICATE THAT AGE MATCHES IN MATERIAL PROPERTIES AND RISK FUNCTION (FULL AGE ADJUSTMENT).

| | | Age in risk function | | | | | |
|---|---|---|---|---|---|---|---|
| Pendulum speed [m/s] | Age in material model [YO] | NFR2+ @ 25 YO [%] | NFR2+ @ 45 YO [%] | NFR2+ @ 65 YO [%] | NFR3+ @ 25 YO [%] | NFR3+ @ 45 YO [%] | NFR3+ @ 65 YO [%] |
| | 25 | **0.0** | | | **0.0** | | |
| 4.0 | 45 | 0.0 | **0.5** | 9.6 | 0.0 | **0.0** | 0.7 |
| | 65 | | | **30.4** | | | **6.3** |
| | 25 | **1.2** | | | **0.0** | | |
| 5.0 | 45 | 2.9 | **34.0** | 89.2 | 0.2 | **8.9** | 64.8 |
| | 65 | | | **99.4** | | | **95.4** |
| | 25 | **9.1** | | | **1.0** | | |
| 5.5 | 45 | 23.6 | **82.4** | 99.7 | 4.9 | **53.4** | 97.4 |
| | 65 | | | **100.0** | | | **100.0** |

***Representativeness of Age-specific Material***

Simulating pendulum impacts at 5.5 m/s with sampled material properties representing population variability at 25 YO, 45 YO, and 65 YO produced histograms of NFR2+ risks (Fig. 10), NFR3+ risks (Fig. 11) and NFR4+ risks (Fig. C 1); all show that the risk increases with age. The variability in material properties in general produced a large range of risk values. For example, most 25 YO material properties resulted in predicted NFR2+ risks below 10%, but the tail of the distribution still reached 100% risk (Fig. 10).

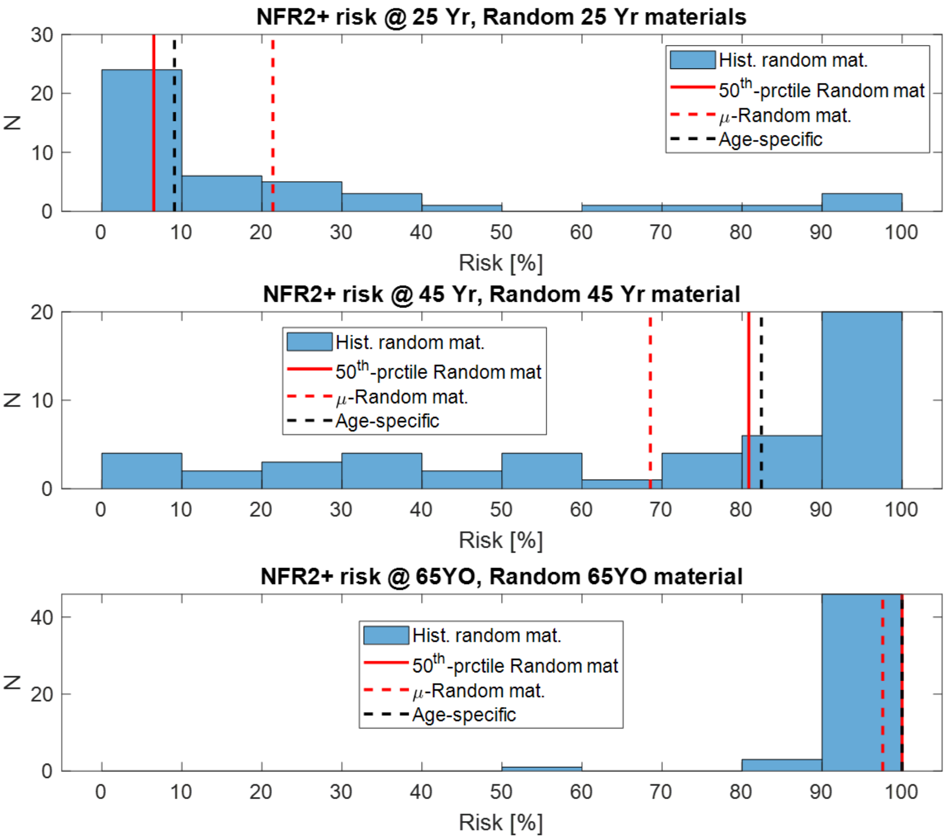


Fig. 10. Histograms of NFR2+ risks Top: 25 YO, Middle: 45 YO, Bottom: 65 YO. Red solid line: 50th percentile value of risk in the sample, Red dashed: mean value, Black dashed: Risk from age-specific material.

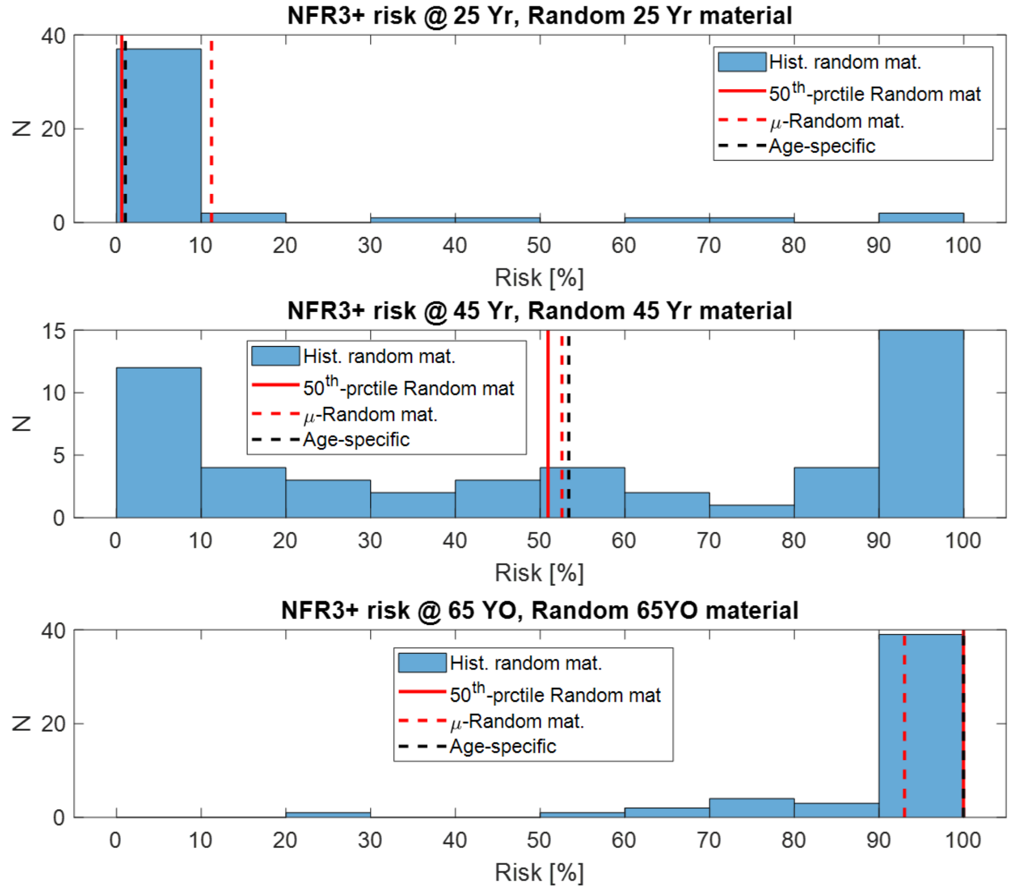


Fig. 11. Histograms of NFR3+ risks Top: 25 YO, Middle: 45 YO, Bottom: 65 YO. Red solid line: 50th percentile value of risk in the sample, Red dashed: mean value, Black dashed: Risk from age-specific material.

Similarly, NFR3+ for 45 YO materials (Fig. 11) ranged from 0 – 100%, with most of the results being at either 0% or 100%. As the resulting distributions of risks in general were skewed, the risk prediction obtained by the corresponding age-specific material did not generally coincide with the mean risk, but was often closer to the median risk magnitude for the corresponding age (Fig. 10, Fig. 11, Fig. C 1).

## IV. DISCUSSION

This study examined the effect of age-adjusting rib cortical bone material properties, in addition to the age covariate in the strain-based risk function, on age-dependent probabilistic rib fracture risk prediction in HBMs. The representativeness of age-adjusted material properties for the age cohort was examined, which is important as there is substantial inter-individual variability. The results show that applying age adjustment only in the strain-based risk function (partial age adjustment) is not equivalent to also incorporating age effects in the material model, as material ageing influences the overall stiffness of the ribs, and thus also the predicted rib strains used in risk calculations. When material variability is considered, age-specific material properties represent the median rather than the mean response, consistent with previous observations that average biomechanical models may yield non-average predictions [31].

### *Age-dependent Rib Cortical Bone Material Behaviour*

For the age of 70 years, the material properties estimated from the current study resulted in tensile Young's modulus of 13.4 GPa and yield stress of 69.2 MPa (compressive: Young's modulus 11.8 GPa, yield stress 155.9 MPa), which is close to values reported by [22], who used the same tensile test data source but analysed in a different way. Differences relative to other published values (TABLE I) reflect not only biological variability, but also differences in data processing, as prior studies typically derived scalar parameters from engineering stress–strain curves and linear regression on separate parameters for age trends, whereas the present approach operates directly on true stress–strain curve shape and non-linear regression. The latter approach naturally keeps the covariance of individual material parameters (e.g. Young's modulus and yield stress), as stress-strain curves defines both.

A primary motivation for applying PCA was to enable curve-level analysis of ageing effects: capturing elastic, yield, and post-yield behaviour simultaneously rather than through uncoupled scalar parameters. Two PCs were sufficient to describe nearly all experimentally observed variability, resulting in a compact age-scalable representation. The PC scores versus age trends in the current study are broadly consistent with experimental observations reported in the literature. The non-linear age trends identified here were partly motivated by minimising cross-validated RMSE and partly by earlier experimental observations showing characteristic decade-averaged stress–strain curves that stiffen toward mid-age and decrease again at older ages [18–19]. In addition, similar age-trends have been indicated in rib stiffness and peak force before fracture in rib bending tests [29], and the contribution of material property trends with age to this behaviour can be explored in future work. However, in the light of inter-individual variability, the regression trends were generally weak, particularly for compressive behaviour where the available dataset was smaller. It is therefore possible that other age trends could emerge if additional reference data were made available in future work.

***Inter-individual Variability and Interpretation of Age-specific Material Properties***

After controlling for age, the inter-individual variability in rib cortical bone material behaviour is still large and persists across ages and loading directions. The PCA-based formulation enabled explicit representation of this variability through random sampling of regression residuals. Given the limited sample size, residuals were modelled as normally distributed for practical stochastic sampling. Random sampling was truncated based on resulting Young's modulus to exclude non-physical curve realisations. Alternative strategies, such as direct empirical residual sampling, may be advantageous as larger experimental datasets become available.

When this variability was represented in pendulum impact simulations, predicted rib fracture risks spanned wide and often skewed distributions at each age, frequently saturating at low or high risk, see Fig. 10,Fig. *11*. Under such conditions, the mean risk is not necessarily representative of the risk for an average individual. Consistent with this, risk predicted using age-specific material properties based on regression trends did not generally coincide with the population mean but was often closer to the median.

Age-specific material properties should therefore be interpreted as representing typical age-dependent material response rather than population-average fracture risk. Accounting for material variability, together with other sources of variability relevant to HBM rib fracture risk [26], remains an important topic for future work. This is particularly important in the context of HBM validation against PMHS experiment or field injury outcomes (accident reconstructions) as this variability is expected to also underlie such reference data even when age and anthropometry are controlled.

***Implications for Strain-based Rib Fracture Risk Prediction and Assessment Applications***

The results of this study demonstrate that applying age adjustment only through a strain-based risk function (partial age adjustment) is not equivalent to also incorporating age effects in the material model (full age adjustment). Cortical bone material properties directly influence the rib stiffness, and as such the strain response under load, and because the strain-to-risk relationship is non-linear, even moderate changes in strain can result in large differences in predicted fracture probability.

In rib bending simulations, full age adjustment produced larger reductions in force to the fracture-risk threshold with increasing age than partial age adjustment. In the pendulum impact simulations, the same modelling inconsistency produced systematic shifts in predicted risk across ages. Partial age adjustment consistently predicted higher risks for younger ages (25 vs. 45 YO) and lower risk for higher ages (45 vs. 65 YO), TABLE III, when compared to full age adjustment. These results indicate that material ageing and risk-function ageing address different aspects of age dependence: the former governs strain development, while the latter governs failure tolerance.

A further consideration regarding the simulations where the age effect is only partly adjusted, is that this approach is a convenient computational simplification [15][32]: fracture risks for different ages can be evaluated using the same predicted rib strains without re-running simulations. Updating also the material properties for a full age adjustment requires new simulations to predict updated rib strains at each age analysed. Hence there is a trade-off between computational cost and age adjustment strategy, and the results of the present study provide a basis for informed choices.

Whether age-adjusting rib cortical bone material properties is necessary therefore depends on the application. If the assessment objective is to address fracture risk for elderly occupants specifically, age-adjusting material properties in addition to the risk function is likely an important step towards achieving more representative predictions. Strain-based rib fracture risk predictions are sensitive to material properties, and standardisation of rib cortical bone material properties (together with other properties influential for predicted risk) across HBMs would be an important step toward consistency in predicted risk magnitudes between HBMs used in assessments.

***Limitations and Methodological Considerations***

Several limitations of the present study should be considered when interpreting the results. First, the effects of full vs. partial age adjustment was limited to two simplified anterior-posterior loading scenarios using only a single HBM. It is possible that the effect of full age adjustment can be both smaller or greater, depending on HBM and simulated scenario. However, as material properties directly influence rib model structural responses, it is likely that the systematic shifts identified here will remain if the analysis is expanded to more HBMs and scenarios, although magnitude of effects may vary.

Secondly, strain-rate effects were incorporated using Cowper–Symonds scaling with age-independent parameters that were manually calibrated to achieve reasonable agreement with experimental stress–strain curves across ages, strain rates, and loading modes. Quantitative error metrics and uncertainty bounds were not established due to limited age-matched experimental data across strain rates.

Finally, the study focused solely on rib cortical bone material properties and their influence on strain-based rib fracture risk. Other thoracic factors, such as rib geometry, cortical bone thickness, and costal cartilage calcification, were not varied and may have interacting age, body size, and sex effects on rib fracture risks [33][34]. Addressing age trends, sex effects, and inter-individual variability in these factors remains an important topic for future work, where age trends and variability in material properties could be included through the modelling proposed in this study.

## V. CONCLUSIONS

Applying age adjustment for strain-based rib fracture risk predictions only through an age co-variate in the injury risk function is not equivalent to also incorporating age effects in the rib cortical bone material model parameters, as changing the material properties alters the strain response that in turn governs fracture risk. Only considering age in the injury risk function results in rib fracture risk predictions that are higher for younger ages and lower for older ages, when compared to age-adjusting also the material model parameters.

Representation of inter-individual material variability showed that predicted rib fracture risks vary widely across ages, typically from zero to 100% risk, and that age-specific material models tend to predict typical (median) rather than population-average (mean) risk.

Whether age-adjusting material properties is necessary for probabilistic rib fracture risk prediction with HBMs depends on the application, but neglecting material ageing introduces systematic shifts in predicted age-dependent risk. The proposed curve-based material parametrisation provides a practical approach for incorporating age effects and variability in HBM-based assessments. Material cards are available upon request.

## VI. ACKNOWLEDGEMENTS

The work performed in this study was funded by FFI-Strategic Vehicle Research and Innovation, by Vinnova – Sweden's Innovation Agency, the Swedish Energy Agency, the Swedish Transport Administration and the Swedish vehicle industry. The work was carried out at SAFER – Vehicle and Traffic Safety Centre at Chalmers, Sweden. Generative artificial intelligence (ChatGPT 5.2) was used to support language editing. All scientific content, interpretations, and conclusions were developed, reviewed, and validated by the authors, who take full responsibility for the accuracy and integrity of the work.

## VII. REFERENCES

[1] Östling, M., Jeppsson, H. and Forman, J. (2024) Injury observations in high-exposure, low-severity frontal car crashes – a GIDAS investigation. Proceedings of the IRCOBI Conference, 2024, Stockholm, Sweden.

[2] Forman, J., Jin, R., Östling, M. and Jeppsson, H. (2025) Collision, occupant, and injury characteristics in low-to-moderate speed frontal collisions – an examination of U.S. field data from 2017–2022. Proceedings of the IRCOBI Conference, 2025, Vilnius, Lithuania.

[3] Forman, J., *et al.* (2019) Automobile injury trends in the contemporary fleet: belted occupants in frontal collisions. Traffic Injury Prevention, **20**(6): pp.607–612.

[4] Carter, P. M., Flannagan, C. A. C., Reed, M. P., Cunningham, R. M. and Rupp, J. D. (2014) Comparing the effects of age, BMI and gender on severe injury (AIS 3+) in motor-vehicle crashes. Accident Analysis and Prevention, **72**: pp.146–160.

[5] Kent, R. and Patrie, J. (2005) Chest deflection tolerance to blunt anterior loading is sensitive to age but not load distribution. Forensic Science International, **149**: pp.121–128.

[6] Brumbelow, M. L. and Farmer, C. M. (2013) Real-world injury patterns associated with Hybrid III sternal deflections in frontal crash tests. Traffic Injury Prevention, **14**(8): pp.807–815.

[7] Brumbelow, M. L., Jermakian, J. S. and Arbelaez, R. A. (2022) Predicting real-world thoracic injury using THOR and Hybrid III crash tests. Proceedings of the IRCOBI Conference, 2022, Porto, Portugal, pp.264–287.

[8] Kent, R., Patrie, J. and Benson, N. (2003) The Hybrid III dummy as a discriminator of injurious and non-injurious restraint loading. Annals of Advances in Automotive Medicine, **47**: pp.51–75.

[9] Pipkorn, B., Jakobsson, L., Iraeus, J. and Östh, J. (2023) The SAFER HBM – a human body model for seamless integrated occupant analysis for all road users. Proceedings of the International Technical Conference on the Enhanced Safety of Vehicles (ESV), 2023, Yokohama, Japan.

[10] Matsuda, T., Kobayashi, N., Fujita, N. and Kitagawa, Y. (2023) Development of a human body model (THUMS version 7) to simulate kinematics and injuries of reclined occupants in frontal collisions. Proceedings of the International Technical Conference on the Enhanced Safety of Vehicles (ESV), 2023, Yokohama, Japan.

[11] John, J., Klug, C., Kranjec, M., Svenning, E. and Iraeus, J. (2022) Hello, world! VIVA+: a human body model lineup to evaluate sex-differences in crash protection. Frontiers in Bioengineering and Biotechnology, **10**: p.918904.

[12] Gayzik, F. S., Moreno, D. P., Vavalle, N. A., Rhyne, A. C. and Stitzel, J. D. (2012) Development of a full human body finite element model for blunt injury prediction utilizing a multi-modality medical imaging protocol. Proceedings of the International LS-DYNA Users Conference, 2012, Detroit, MI, USA, pp.1–14.

[13] Robinson, A., Von Kleeck, B. W. and Gayzik, F. S. (2023) Development and preliminary validation of computationally efficient and detailed 50th percentile female human body models. Accident Analysis and Prevention, **190**: p.107182.

[14] Trosseille, X., Baudrit, P., Leport, T. and Vallancien, G. (2008) Rib cage strain pattern as a function of chest loading configuration. Stapp Car Crash Journal, **52**: pp.205–231.

[15] Forman, J., Kent, R. W., Mroz, K., Pipkorn, B., Boström, O. and Segui-Gomez, M. (2012) Predicting rib fracture risk with whole-body finite element models: development and preliminary evaluation of a probabilistic analytical framework. Annals of Advances in Automotive Medicine, **56**: pp.109–124.

[16] Forman, J., Kulkarni, S., Perez Rapela, D., Mukherjee, S., Panzer, M. and Hallman, J. (2022) A method for thoracic injury risk function development for human body models. Proceedings of the IRCOBI Conference, 2022, Porto, Portugal.

[17] Larsson, K.-J., Blennow, A., Iraeus, J., Pipkorn, B. and Lubbe, N. (2021) Rib cortical bone fracture risk as a function of age and rib strain: updated injury prediction using finite element human body models. Frontiers in Bioengineering and Biotechnology, **9**: p.677768.

[18] Katzenberger, M. J., Albert, D. L., Agnew, A. M. and Kemper, A. R. (2020) Effects of sex, age, and two loading rates on the tensile material properties of human rib cortical bone. Journal of the Mechanical Behavior of Biomedical Materials, **102**: p.103410.

[19] Albert, D. L., Katzenberger, M. J., Agnew, A. M. and Kemper, A. R. (2021) A comparison of rib cortical bone compressive and tensile material properties: trends with age, sex, and loading rate. Journal of the Mechanical Behavior of Biomedical Materials, **122**: p.104668.

[20] Jin, X., *et al.* (2018) Development and validation of whole-body finite element occupant and pedestrian models of a 70-year-old female. Proceedings of the IRCOBI Conference, 2018, Athens, Greece.

[21] Schoell, S. L., Weaver, A. A., Vavalle, N. A. and Stitzel, J. D. (2015) Age- and sex-specific thorax finite element model development and simulation. Traffic Injury Prevention, **16**: pp.57–65.

[22] Von Kleeck, B. W., Hostetler, Z., Fleischmann, K., Weaver, A. A. and Gayzik, F. S. (2022) Age targeted human body models indicate increased thoracic injury risk with aging. Traffic Injury Prevention, **23**: pp.1–6.

[23] Euro NCAP (2025) Crash Protection Frontal Impact Protocol Version 1.0. www.euroncap.com [06 Apr 2026].

[24] Euro NCAP (2025) Qualification Procedure for Human Body Models, Technical Bulletin CP 550, Version 1.1. www.euroncap.com [06 Apr 2026].

[25] OpenVT “HBM4VT Validation Catalogue”, https://openvt.eu/EuroNCAP/hbm4vt-validation-catalogue [15 Feb 2026].

[26] Larsson, K.-J., Iraeus, J., Holcombe, S. and Pipkorn, B. (2023) Influences of human thorax variability on population rib fracture risk prediction using human body models. Frontiers in Bioengineering and Biotechnology, **11**: p.1154272.

[27] Cook, D., Julias, M. and Nauman, E. (2014) Biological variability in biomechanical engineering research: significance and meta-analysis of current modeling practices. Journal of Biomechanics, **47**(6): pp.1241–1250.

[28] Iraeus, J., Brynskog, E. and John, J., *et al.* Development of SAFER HBM v11. Chalmers University of Technology. Report 2024:06.

[29] Agnew, A. M., *et al.* (2018) Sources of variability in structural bending response of pediatric and adult human ribs in dynamic frontal impacts. Stapp Car Crash Journal, **62**: pp.119–192.

[30] Iraeus, J., *et al.* (2019) Detailed subject-specific FE rib modeling for fracture prediction. Traffic Injury Prevention, **20**(S2): pp.88–95.

[31] Cook, D. D. and Robertson, D. J. (2016) The generic modeling fallacy: average biomechanical models often produce non-average results. Journal of Biomechanics, **49**(15): pp.3609–3615.

[32] Guleyupoglu, B., Koya, B., Barnard, R. and Gayzik, F. S. (2018) Failed rib region prediction in a human body model during crash events with pre-crash braking. Traffic Injury Prevention, **19**(S1): pp.S37–S43.

[33] Holcombe, S. A., Ejima, S. and Wang, S. C. (2017) Calcification of costal cartilage in the adult rib cage. Proceedings of the IRCOBI Conference, 2017, Antwerp, Belgium, pp.737–744.

[34] Holcombe, S. A., Huang, Y. and Derstine, B. A. (2024) Population trends in human rib cross-sectional shapes. Journal of Anatomy, **244**: pp.792–802.

## VIII. APPENDIX A – CORRELATION ANALYSIS

PC score correlations between computed PCs for Fast and Slow curves are shown for tensile tests in Fig. A. 1 and for compressive tests in Fig. A. 2.

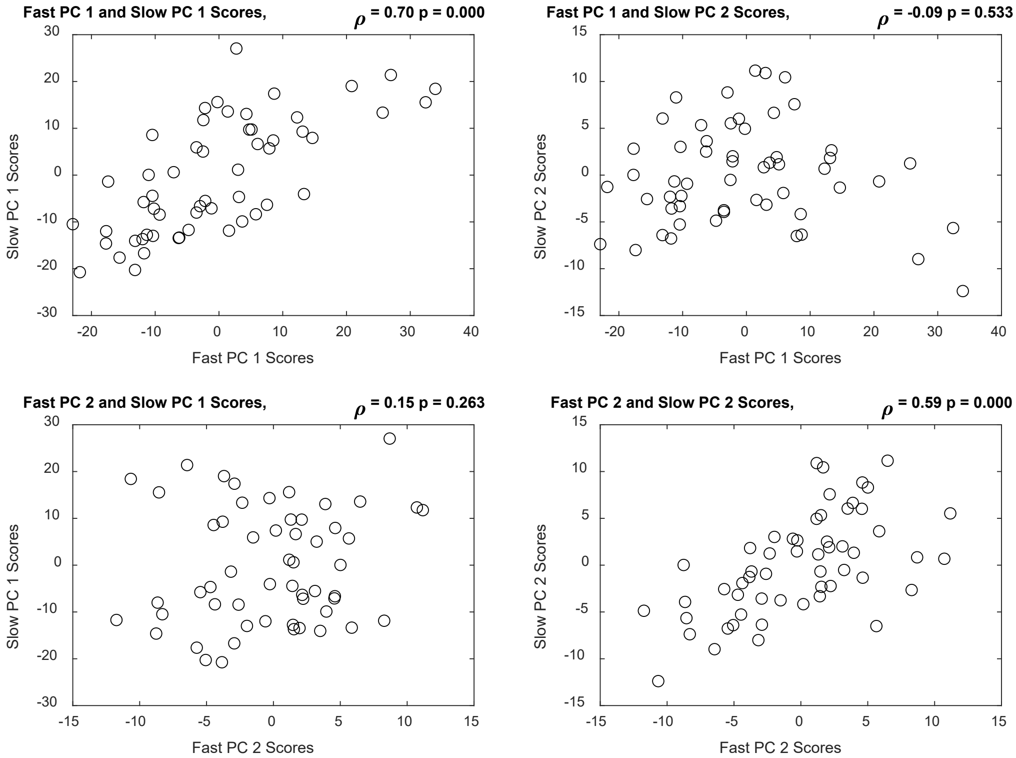


Fig. A. 1. Tensile tests: Correlation for PC scores across loading rates

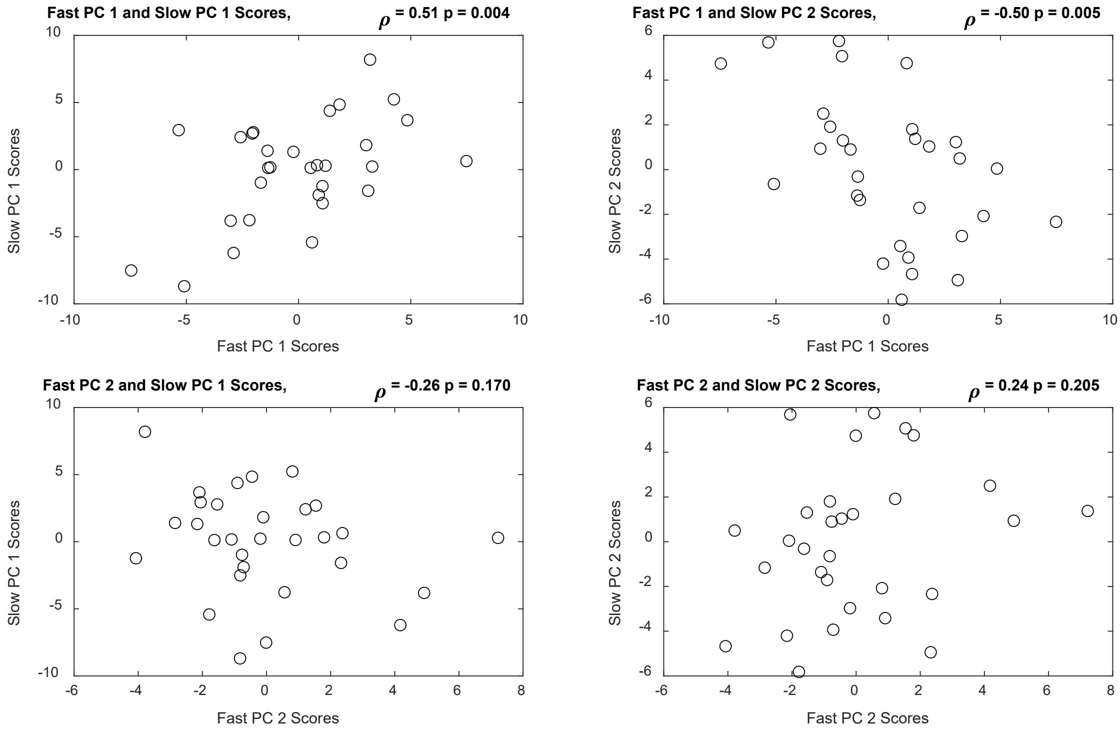


Fig. A. 2. Compressive tests: Correlation for PC scores across loading rates

## IX. APPENDIX B

Figs. B 1–Fig. B 4 show material model stress and strain response at Fast and Slow rates for ages 20, 30, …, 90 YO.

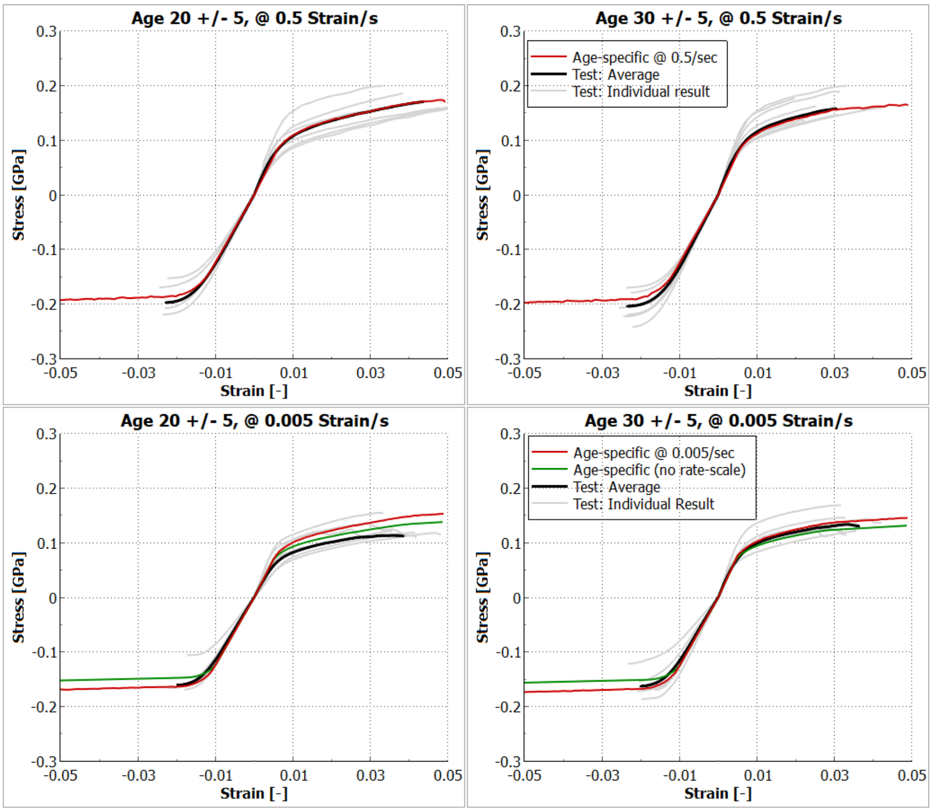


Fig. B1. Tensile and compressive stress-strain curves computed from age-specific material properties at 20 and 30 YO, including test curves from ± 5 years [18–19]. Top: Fast, bottom: Slow and quasistatic (no rate-scale)

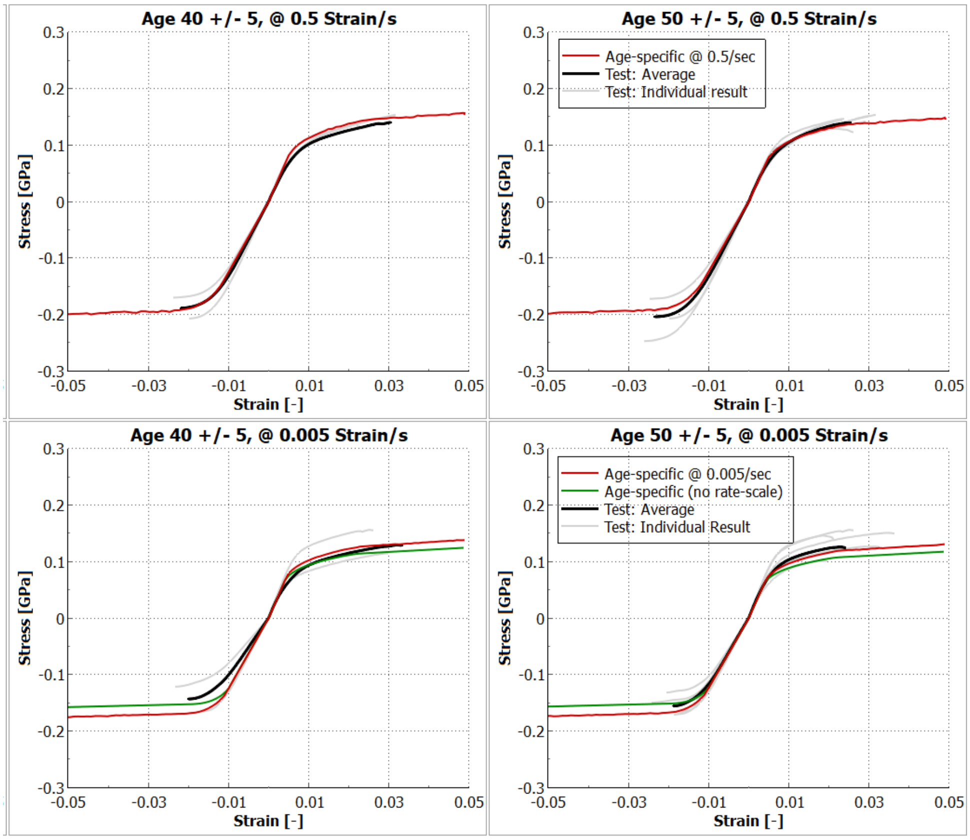

Fig. B 2. Tensile and compressive stress-strain curves computed from age-specific material properties at 40 and 50 YO, including test curves from ± 5 years [18–19]. Top: Fast, bottom: Slow and quasistatic (no rate-scale).

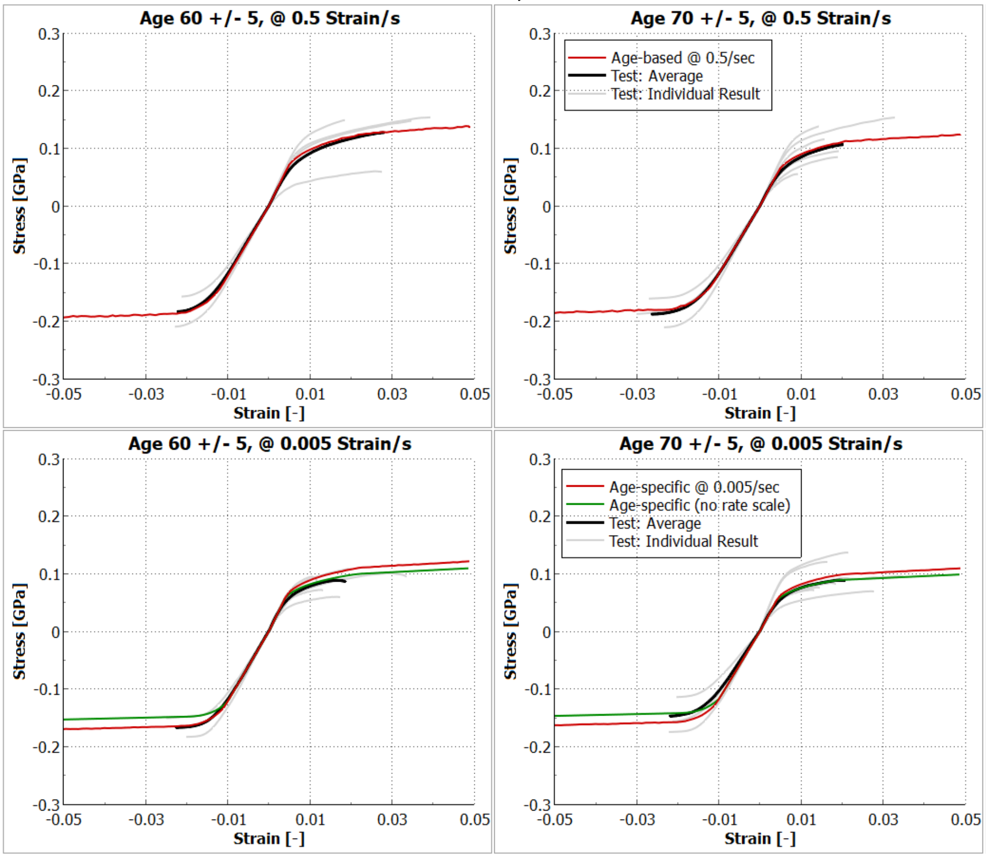


Fig. B 3. Tensile and compressive stress-strain curves computed from age-specific material properties at 60 and 70 YO, including test curves from ± 5 years [18–19]. Top: Fast, bottom: Slow and quasistatic (no rate-scale).

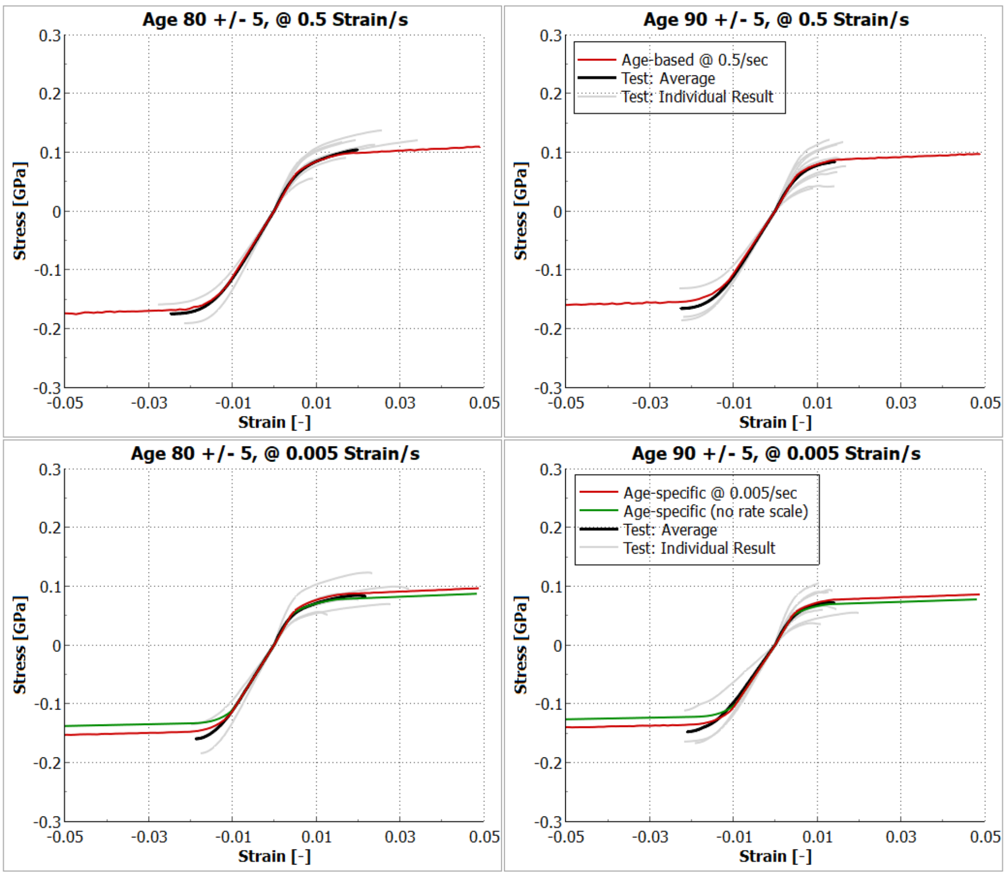

Fig. B 4. Tensile and compressive stress-strain curves computed from age-specific material properties at 80 and 90 YO, including test curves from ± 5 years [18–19]. Top: Fast, bottom: Slow and quasistatic (no rate-scale).

## X. APPENDIX C

The NFR4+ risks from 5.5 m/s pendulum impact calculated with random material properties, as well as with age-specific material properties are shown in Fig. C 1.

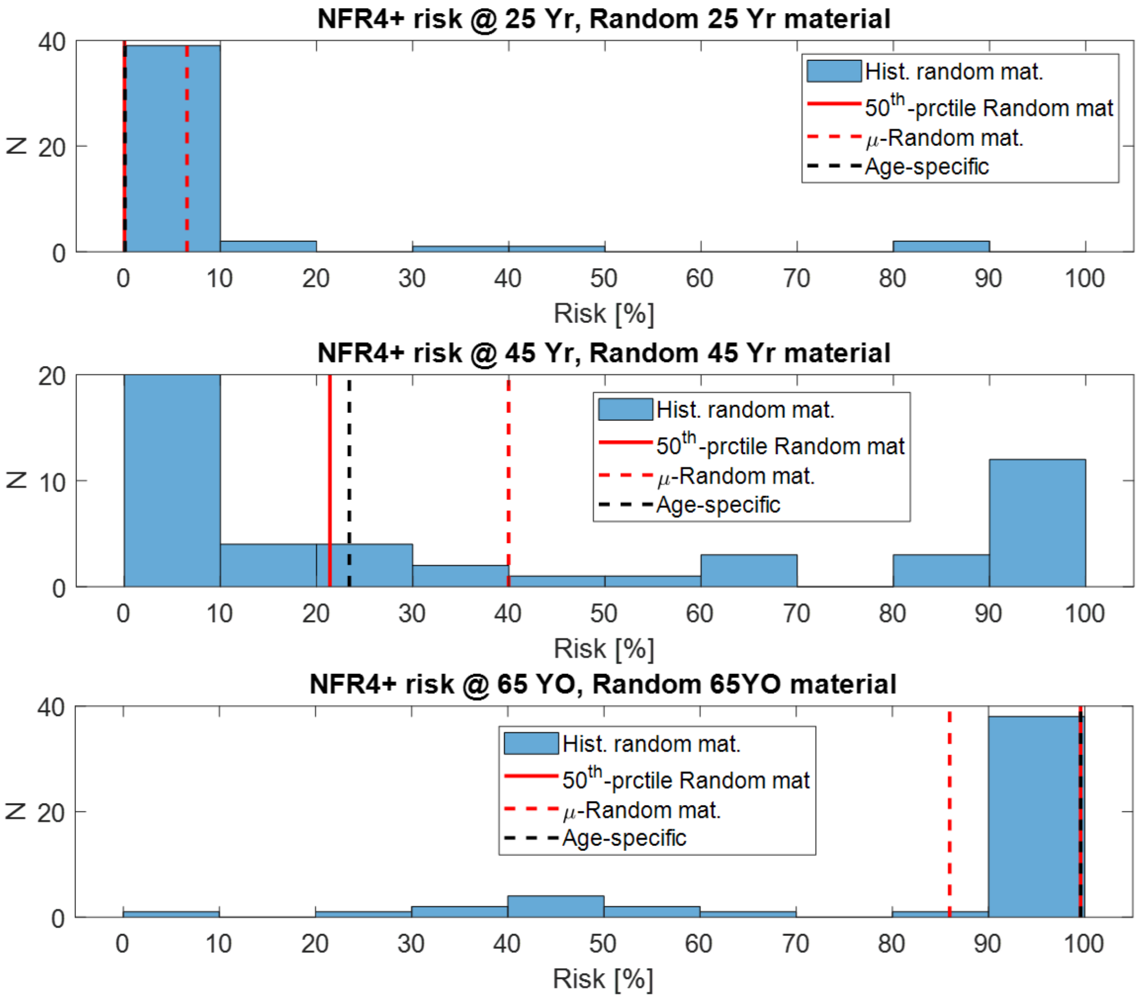


Fig. C 1. Histograms of NFR4+ risks Top: 25 YO, Middle: 45 YO, Bottom: 65 YO. Red solid line: 50th percentile value of risk in the sample, Red dashed: mean value, Black dashed: Risk from age-specific material.